

Influence of pressure on the Fermi surface of niobium

J. R. Anderson

University of Maryland, College Park, Maryland 20742

D. A. Papaconstantopoulos

Naval Research Laboratory, Washington, D. C. 20375

J. E. Schirber

Sandia Laboratories, Albuquerque, New Mexico 87115

(Received 5 August 1981)

The effects of pressure on selected de Haas—van Alphen frequencies in niobium have been measured. The frequency shifts, including a relatively large negative shift for the jungle-gym arms, can be explained by a model which uses a Slater-Koster interpolation of augmented-plane-wave $X\alpha$ bands which had been calculated for two lattice spacings.

I. INTRODUCTION

Niobium has the highest transition temperature for an elemental metal and thus is considered a technologically significant material. Since superconductivity depends in part upon the distribution of electrons, it is important to establish a reliable model for the electronic structure of niobium.

Previously we carried out augmented-plane-wave (APW) calculations and de Haas—van Alphen (dHvA) experiments to determine the band structure of niobium and the effect of pressure on the Fermi surface. (This reference will be referred to as I.)¹ The first band-structure calculations for Nb were carried out by Mattheiss.² His results, in general, are still accepted. Since then there have been additional investigations of niobium^{3–5} which have helped to clarify the earlier experiments and the relationship between the electronic structure of niobium and its other physical properties.

We have now obtained additional experimental results from our dHvA measurements of niobium. A striking disagreement between the previously calculated¹ and currently observed pressure derivatives for a prominent sheet of the Fermi surface has been corrected by our new calculations. In the present work we have compared our measurements with APW calculations for both the normal lattice spacing and a 1% reduced spacing. We have learned that an accurate interpolation of the APW energies is necessary in order to make reliable comparisons with Fermi-surface data. A Slater-Koster interpo-

lation scheme,⁶ discussed in Sec. IV, was used for this purpose.

II. EXPERIMENTAL TECHNIQUES

We have obtained the changes in dHvA frequencies with pressure using the standard field modulation technique. The measurements were carried at temperatures between 1.2 and 4 K in both a 55 kOe superconducting solenoid and a 100 kOe split coil. The changes of dHvA frequencies with pressure were determined mainly by the solid-helium-phase-shift technique.⁷ The sample was contained in a beryllium-copper pressure vessel and the pressure was transmitted to the sample by means of solid helium. A few dHvA cycles were measured at fixed pressure; then the pressure was changed and the same dHvA cycles were remeasured to determine the shift of phase. In order to change the pressure, the vessel was raised in the cryostat to allow the solid helium to melt. While the helium was fluid, the pressure was varied and then the helium was resolidified by lowering the pressure vessel in the cryostat. Pressures up to 5 kbar were used in this study. The magnetic field settings were reproduced by measuring the magnetoresistance of the pickup coil.

The samples were [100] and [111] axis single crystals about 3 mm in diameter and 8 mm long with typical resistivity ratios⁸ of about 7000. Before use in the 55 kOe solenoid the samples were

etched slightly with a mixture of 20 vol % HF, 50 vol % HNO₃, and 30 vol % H₂O. For use in the 100 kOe magnet the samples were etched down to about 0.7 mm diameter and a length of about 2 mm.

III. EXPERIMENTAL RESULTS

In order to describe our results on niobium we will refer to the calculations of Mattheiss² for the Fermi-surface notation and use the nomenclature of Karim *et al.*³ for the experimental frequencies. The Fermi surface consists of pieces in two bands. The ν oscillations refer to the third-band ellipsoidal-like hole pockets at N . The α oscillations are considered to result from the arms of the jungle-gym-like Γ -centered third-band surface. The second-band hole octahedron produces oscillations labeled γ_1 which are difficult to see because of the large cyclotron mass of the carriers. The oscillations η correspond to another portion of the jungle gym near the symmetry point H . The low-frequency β oscillations, observed only for magnet-

ic field orientations near [100], have been something of a puzzle and will be discussed later.

In Table I experimental values for pressure derivatives of selected extremal cross sections of the Fermi surface are shown. The cross-sectional areas of the hole ellipsoids at N (ν oscillations) change almost uniformly with pressure at a rate of about 0.1% kbar. This is about three times the compressibility scaling prediction of $2/3K_T$. (The compressibility⁹ $K_T = 5.78 \times 10^{-4}$ kbar⁻¹ at 4 K.) The jungle-gym arm extremal cross section, normal to [100], decreases significantly with pressure in contradiction to the prediction in I. (This value was obtained not only with the solid-helium-phase-shift technique but also by counting dHvA cycles at atmospheric and 4 kbar pressure.)

We were unable to observe sufficiently clean signals from the hole octahedron at our lowest temperatures and highest fields, 1.2 K and 100 kOe, for measurement of the pressure dependence. One large cross section of the jungle gym, centered at H and normal to [111], was studied, but, because slight irreproducible tilting occurred as the pressure was changed, we were able to put only an

TABLE I. Selected extremal cross sections of the Fermi surface and their pressure derivatives.

Normal	Orbit	F (MG)		m^*/m_0		$d \ln A / dP$ (10^{-3} kbar ⁻¹)	
		Expt. ^a	Calc.	Expt. ^a	Calc.	Expt.	Calc.
[001]	$\nu_{1,2}$	66.94	73.5	1.94	0.79	0.9 ± 0.1	0.65
	ν_{3-6}	85.3	99.4	1.96	1.06	1.0 ± 0.1	0.74
	α	14.45	9.0	1.5	0.36	-1.5 ± 0.2	-1.3
	γ_1	104.6	76.0	4.8	2.1		-1.2
[111]	$\nu_{1,3,4}$	67.42	74.4	1.41	0.75	1.0 ± 0.1	0.61
	$\nu_{2,5,6}$	84.9	98.3	2.17	1.06		0.71
	$\eta(H)$	194.2	190	2.7	1.3	< 0.1	0.13
	γ_2^b	86.71	63.7 (42.6) [87.4]	~ 5.5	2.5 (2.5) [0.7]		-1.1 (-2.8) (-0.5)
	γ_1	50.48	30.6	3.8	1.5		-3.0
[110]	ν_{3-6}	69.5	76.8	1.57	0.74		0.64
	ν_1	79.7	84.6	1.58	0.77		0.30
	ν_2	90.10	104.4	2.03	0.96		0.82
	γ_1	78.23	54.9		1.9		-1.6

^aKarim *et al.* (Ref. 3).

^bThe γ_2 oscillations have been attributed³ to a Γ -centered orbit on the jungle gym. The calculations have been made for this orbit. A noncentral orbit on the second-band hole octahedron is another possibility for γ_2 . Calculations for this orbit are enclosed in parentheses. A third possibility is a complicated noncentral orbit around the third-band jungle gym. Calculations for this orbit are enclosed in brackets.

upper limit on the pressure derivative for this frequency as indicated in Table I.

We also looked at the β 's but were unable to obtain reproducible measurements of the change of phase with pressure. These β 's were found to be shifted approximately 90° on the lock-in amplifier relative to the phase of the other dHvA components. In addition, the amplitude of the β oscillations decreased with pressure. (At 1 kbar the amplitude was about half that at atmospheric pressure.) It was suggested³ that the β oscillations are due to quantum interference oscillations¹⁰ and our observations support this. Quantum interference oscillations are expected to be sensitive to orientation. Therefore, the decrease in amplitude with pressure may be a result of a very slight amount of sample tilting.

IV. CALCULATION

Boyer *et al.*¹¹ have carried out self-consistent, nonrelativistic APW calculations using the X_α exchange approximation¹² for the normal lattice constant, $a_0 = 3.3066 \text{ \AA}$, and for a 1% reduced spacing,¹³ $a = 0.99a_0 = 3.2735 \text{ \AA}$. Although the Kohn-Sham form of exchange gave better agreement with Fermi-surface measurements in niobium,¹¹ we decided to use these X_α energies because they were available for two lattice spacings. We expected the X_α calculations to give, at least, reasonable predictions for trends in the pressure derivatives.

The APW calculations were made on a $55 \vec{k}$ -point mesh in $1/48$ of the Brillouin zone. The Slater-Koster (SK) interpolation scheme⁶ was used to fit the APW energies. Our SK fit used an orthonormal basis set of one s , three p , and five d functions; consequently, our nonsymmetrized tight-binding Hamiltonian was a 9×9 . As adjustable parameters we used 44 three-center interaction integrals that included all first, second, and third neighbors. The parameters were determined by a nonlinear least-squares procedure. Symmetry was used to reduce the size of the secular equation at each \vec{k} point resulting from the 9×9 Hamiltonian. The APW energies of the lowest six bands on a uniform grid of $14 \vec{k}$ points in the irreducible wedge ($1/48$) of the body-centered-cubic zone were fitted. In addition from a $55 \vec{k}$ -point grid we included those \vec{k} points along the symmetry lines, Δ , Λ , D , G , and F for the lowest six bands. In order to obtain SK parameters that reflected the correct wave-function character, we also included in the fit

energies from higher bands, seven through nine, at the symmetry points, Γ , H , N , and P . Since we wanted the best fit near the Fermi energy, those energies within approximately 0.1 Ry of the Fermi energy were weighted six times the minimum weight, for example, the weight of a Γ_1 state. The total number of APW energies that was fitted was 250. The rms deviations of our SK energies (six bands at $55 \vec{k}$ points) was about 0.0045 Ry. For bands two and three the rms deviations were less than 0.003 Ry. This was significantly better than the rms error for six bands of 0.0075 Ry that was achieved by Boyer *et al.*¹¹ using an SK interpolation with only 31 parameters. In Table II the SK parameters for both the normal and 1% reduced lattice spacings are presented in the standard SK notation.⁶

Using these SK parameters, we diagonalized the SK Hamiltonian for 1785 \vec{k} points in the irreducible wedge of the Brillouin zone. The tetrahedron method¹⁴ of integration was then used in order to determine the density of states and the Fermi energy. Once the Fermi energy had been determined, cross-sectional areas of the Fermi surface were calculated with high precision by using the tetrahedron method for interpolation.

At this point it may be useful to comment about the appropriate SK mesh size for a reliable determination of Fermi-surface cross sections. Initially we attempted to use the tetrahedron method to interpolate directly from the 55 first-principles points. The results were clearly unsatisfactory. The surface obtained was not smooth and we were unable to carry out meaningful calculations of the jungle-gym cross sections in order to find an extremal area. Therefore, we used SK interpolation to increase the number of \vec{k} points from 55 to 285. Although considerable improvement was obtained, discontinuities remained. Increasing the SK interpolated points to 506 reduced the size of the discontinuities, but acceptable results were produced only with 1785 points. The results we are reporting here were obtained with this last mesh.

The results for cross sections of the Fermi surface are quite similar to those of I. In Fig. 1 the jungle-gym arm cross section as a function of the perpendicular distance from Γ toward H is given for both the normal and 1% reduced lattice spacing. We have converted all our calculated areas A in angstrom^{-2} to frequencies F in megagauss by means of the relation,

$$F(\text{MG}) = A(\text{\AA}^{-2})(1.04728 \times 10^2). \quad (1)$$

TABLE II. Slater-Koster parameters for Nb. The entries are in rydbergs and the notation follows that of Ref. 6 with the abbreviation $d_1 \equiv x^2 - y^2$ and $d_2 \equiv 3z^2 - r^2$.

SK parameters	a_0	$0.99a_0$	SK parameters	a_0	$0.99a_0$	SK parameters	a_0	$0.99a_0$
	On site		Second neighbor			Third neighbor		
$E_{s,s}(000)$	1.2155	1.2964	$E_{s,s}(200)$	-0.0205	-0.0210	$E_{s,s}(220)$	0.0040	0.0019
$E_{x,x}(000)$	1.5348	1.5969	$E_{s,x}(200)$	-0.0841	-0.0994	$E_{s,x}(220)$	-0.0010	-0.0025
$E_{xy,xy}(000)$	0.7909	0.8218	$E_{s,d_2}(002)$	0.0351	0.0437	$E_{s,xy}(220)$	-0.0029	-0.0052
$E_{d_2,d_2}(000)$	0.7452	0.7729	$E_{x,x}(200)$	0.1940	0.2039	$E_{s,d_2}(220)$	0.0062	0.0056
	First neighbor		$E_{y,y}(200)$	-0.0018	-0.0066	$E_{x,x}(220)$	0.0081	0.0102
$E_{s,s}(111)$	-0.1113	-0.1144	$E_{x,xy}(020)$	-0.0038	-0.0081	$E_{x,x}(022)$	0.0034	-0.0002
$E_{s,x}(111)$	-0.0663	-0.0649	$E_{z,d_2}(002)$	0.0757	0.0812	$E_{x,y}(220)$	0.0093	0.0114
$E_{s,xy}(111)$	0.0561	0.0537	$E_{xy,xy}(200)$	0.0059	0.0067	$E_{x,xy}(220)$	0.0018	0.0026
$E_{x,x}(111)$	0.0831	0.0847	$E_{xy,xy}(002)$	0.0003	-0.0016	$E_{x,xy}(022)$	-0.0004	-0.0039
$E_{x,y}(111)$	0.0384	0.0406	$E_{d_2,d_2}(002)$	-0.0569	-0.0602	$E_{z,d_2}(022)$	-0.0008	-0.0008
$E_{x,xy}(111)$	0.0424	0.0412	$E_{d_1,d_1}(002)$	0.0036	0.0048	$E_{z,d_1}(022)$	0.0050	0.0027
$E_{x,yz}(111)$	0.0489	0.0513				$E_{xy,xy}(220)$	0.0008	0.0017
$E_{x,d_1}(111)$	-0.0223	-0.0202				$E_{xy,xy}(022)$	0.0014	0.0020
$E_{xy,xy}(111)$	-0.0226	-0.0239				$E_{xy,xz}(022)$	0.0001	0.0009
$E_{xy,xz}(111)$	-0.0356	-0.0372				$E_{yz,d_2}(220)$	-0.0044	-0.0044
$E_{xy,d_2}(111)$	-0.0166	-0.0181				$E_{d_2,d_2}(220)$	0.0050	0.0047
$E_{d_2,d_2}(111)$	0.0295	0.0312				$E_{d_1,d_1}(220)$	-0.0055	-0.0041

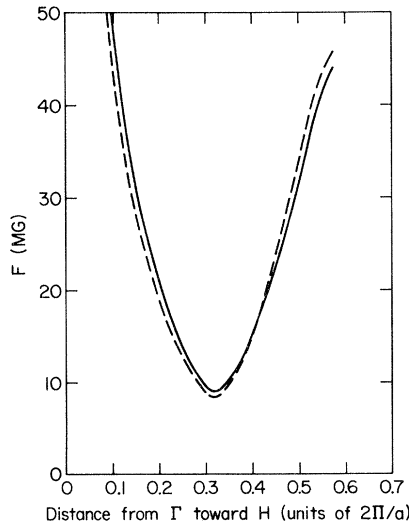


FIG. 1. Calculated cross-sectional areas (in frequency units) of the jungle-gym arms normal to [100]. The axis of the abscissa is the perpendicular distance from Γ to the cross section. Results for the normal lattice spacing (a_0) are given by the solid curve. The dashed curve represents the reduced spacing ($0.99a_0$).

From Fig. 1 we observe that the extremal area, at a distance of about 0.31 ($2\pi/a$) from Γ , decreases with pressure. The calculated pressure derivative (Table I) is in excellent agreement with the measured change in the dHvA frequency of the α oscillations with pressure. We also see, however, that our graphical interpolation in I could have been in error since at about 0.4 ($2\pi/a$) the curves corresponding to the two lattice spacings cross. Thus even the sign of the pressure derivative could be affected by an error in determining the position of the minimum cross section.

For the hole "ellipsoids" at N the calculations fit quite well the general shape as shown by the variation of extremal cross section (or dHvA frequency) with orientation in Fig. 2. For example, there is a minimum frequency at about 30° from [100] in a (110) plane, which agrees with the experimental results.³ The calculated magnitudes of the frequencies are larger than the experimental values by about 10%, however. The calculated pressure derivatives given in Table I are somewhat smaller than the measured results although when one takes into account the uncertainties in the calculation and the experimental errors, the agreement is

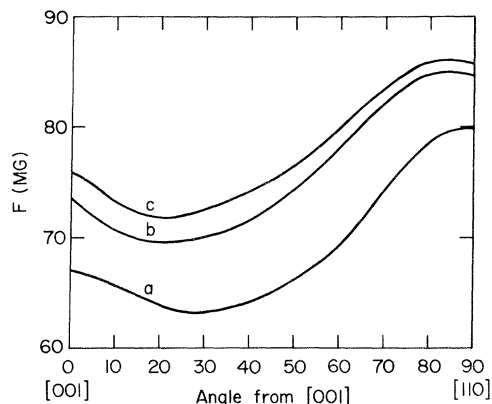


FIG. 2. Orientation dependence of the cross-sectional areas (in frequency units) of the third-band hole ellipsoids. The angle of the normal from [001] is given by the axis of the abscissa. *a*, experimental values; *b*, calculated for the normal lattice spacing a_0 ; *c*, calculated for $0.99a_0$.

reasonable.

The best fit to the dHvA frequencies, approximately a 2% difference, was found for the jungle-gym cross section centered at H and normal to [111]. The calculated value for the pressure derivative is small but slightly larger than the upper limit predicted by our experiment. Again in view of the uncertainties in the calculation the agreement is satisfactory. The fact that the portion of the jungle gym near H is relatively insensitive to pressure can also be seen from the (100) sections in Fig. 1. We have presented some additional calculated pressure derivatives of cross-sectional areas (frequencies) in Table I although we have no experimental values for them at this time.

V. CONCLUSIONS

We have improved and expanded upon our preliminary measurements¹ of derivatives of dHvA frequencies with pressure. We found a large decrease in frequency with pressure for the jungle-gym arms (α oscillations) although the APW calculations in I predicted an increase. This result as well as our other measurements has been interpreted with the aid of a Slater-Koster interpolation of self-consistent APW calculations with the X_α form for exchange.¹² We found that it was necessary to use 1785 SK interpolated points in 1/48 of the Brillouin zone in order to produce a smooth Fermi surface. Once this was done we were able to obtain reasonable agreement with the measured pressure derivatives. The previous discrepancy in the jungle-gym arm cross section occurred, we believe, because of the crude graphical interpolation from only 14 APW points that was used in I and not because of problems with the APW calculation or the form of exchange and correlation chosen.

ACKNOWLEDGMENTS

We wish to give special thanks to D. L. Overmyer for help with the experiment and to Dr. L. L. Boyer, Dr. W. E. Pickett, and Dr. B. M. Klein for helpful discussions regarding the Fermi-surface calculations. The support of the University of Maryland Computer Science Center and, in particular, the assistance of H. J. Breitenlohner, is gratefully acknowledged. The experimental work was supported in part by the U.S. Department of Energy under Contract No. DE-AC04-76-DP00789. The experimental work was done at a Department of Energy facility.

¹J. R. Anderson, D. A. Papaconstantopoulos, J. W. McCaffrey, and J. E. Schirber, Phys. Ref. B **7**, 5115 (1973).

²L. F. Mattheiss, Phys. Rev. **139**, A1893 (1965).

³D. P. Karim, J. B. Ketterson, and G. W. Crabtree, J. Low Temp. Phys. **30**, 389 (1978).

⁴N. Elyashar and D. D. Koelling, Phys. Rev. B **15**, 3620 (1977); **13**, 5362 (1976).

⁵S. Wakoh, Y. Kubo, and J. Yamashita, J. Phys. Soc. Jpn. **38**, 416 (1975).

⁶J. C. Slater and G. F. Koster, Phys. Rev. **94**, 1498 (1954).

⁷J. E. Schirber and R. L. White, J. Low Temp. Phys.

23, 445 (1976).

⁸The samples were furnished by the late Dr. R. E. Reed of Oak Ridge National Laboratory.

⁹K. J. Carroll, J. Appl. Phys. **36**, 3689 (1965).

¹⁰R. W. Stark and C. B. Friedberg, J. Low Temp. Phys. **14**, 111 (1974).

¹¹L. L. Boyer, D. A. Papaconstantopoulos, and B. M. Klein, Phys. Rev. B **15**, 3685 (1977).

¹²K. Schwarz, Phys. Rev. B **5**, 2466 (1972).

¹³D. A. Papaconstantopoulos, B. M. Klein, and J. W. McCaffrey, unpublished.

¹⁴G. Lehmann and M. Taut, Phys. Status Solidi **54**, 469 (1972).